Spin dephasing in quantum wires

S. Pramanik and S. Bandyopadhyay*

Department of Electrical Engineering, Virginia Commonwealth University, Richmond, Virginia 23284, USA

M. Cahay

Department of Electrical and Computer Engineering and Computer Science, University of Cincinnati, Cincinnati, Ohio 45221, USA

We study high-field spin transport in a quantum wire using a semiclassical approach. Spin dephasing (or spin depolarization) in the wire is caused by D'yakonov-Perel' relaxation associated with bulk inversion asymmetry (Dresselhaus spin-orbit coupling) and structural inversion asymmetry (Rashba spin-orbit coupling). The depolarization rate is found to depend strongly on the initial polarization of the spin. If the initial polarization is along the axis of the wire, the spin depolarizes ~100 times slower compared to the case when the initial polarization is transverse to the wire axis. We also find that in the range 4.2–50 K, temperature has a weak influence and the driving electric field has a strong influence on the depolarization rate. The steady state distribution of the spin components parallel and transverse to the wire axis also depend on the initial polarization. If the initial polarization is along the wire axis, then the steady state distribution of both components is a flat-topped uniform distribution, whereas if the initial polarization is transverse to the wire axis, then the distribution of the longitudinal component resembles a Gaussian, and the distribution of the transverse component is U shaped.

I. INTRODUCTION

There is considerable current interest in spin transport in quantum confined structure because of the advent of the field of spintronics.[1-4] A number of device proposals advocate the use of the spin degree of freedom of an electron (as opposed to the charge degree of freedom) to realize electronic devices such as transistors,[5] diodes,[6] solar cells,[7] filters,[8] and stub tuners.[9] Additionally, spin is nowadays preferred to charge for encoding qubits in quantum logic gates[10-13] because of the much longer spin coherence time in semiconductors[14,15] compared to charge coherence time.[16]

In this paper, we study electron spin transport in quasi one-dimensional structures. In the past, single particle ballistic models[9,17-19] were employed to study spin transport. They are fully quantum mechanical, but do not account for any scattering or spin dephasing. More recently, Cahay and Bandyopadhyay have treated spin dephasing via elastic impurity scattering within a fully quantum mechanical model.[20] However, they do not account for spin dephasing via *inelastic* (phase-breaking) scattering mechanisms which are important at elevated temperatures and high electric fields.

As far as classical models are concerned, a number of studies used a drift-diffusion type approach to model spin transport and spin dephasing at elevated temperatures and moderate electric fields.[21-23] "Spin-up" and "spin-down" electrons are treated similar to electrons and holes in conventional bipolar transport. Spin dephasing is treated by a spin relaxation term that describes coupling between the "spin-up" and "spin-down" electrons similar to the generation-recombination term describing coupling between electrons and holes in bipolar transport. The inadequacy of these models has been pointed out by Saikin *et al.*[24] Apart for the fact that a relaxation time approximation does not fully capture the physics of spin dephasing (even if different relaxation

times are used to describe different processes[25]), the drift-diffusion formalism is invalid at relatively high electric fields when transport nonlinearities become important.[26] Nonlinearities in spin transport have been observed experimentally.[27,28] Furthermore, these models cannot treat coherence effects arising from superposition of spin-up and spin-down states. Recently, such superpositions were treated in a Bloch equation approach[29] and a generalized drift-diffusion type approach derived from the Boltzmann transport equation.[30] These later models are still somewhat inadequate in that they do not treat the momentum dependence of the spin-orbit coupling (the primary cause of spin dephasing) self-consistently.

In reality, the temporal evolution of spin and the temporal evolution of the momentum of an electron cannot be separated. The dephasing (or depolarization) rates are functionals of the electron distribution function in momentum space which continuously evolves with time when an electric field is applied to drive transport. Thus, the dephasing rate is a dynamic variable that needs to be treated self-consistently in step with the dynamic evolution of the electron's momentum. Such situations are best treated by Monte Carlo simulation, which has been recently adopted by a number of groups to study spin transport in quasi-two-dimensional structures.[31,24] In this paper, we extend this approach to quasi one-dimensional structures using a multisubband Monte Carlo simulator.

This paper is organized as follows. In the next section, we describe the theory followed by results and discussions in Sec. III. Finally, we conclude in Sec. IV.

II. THEORY

Consider a quasi-one-dimensional semiconductor structure shown in Fig. 1. An electric field E_x is applied along the
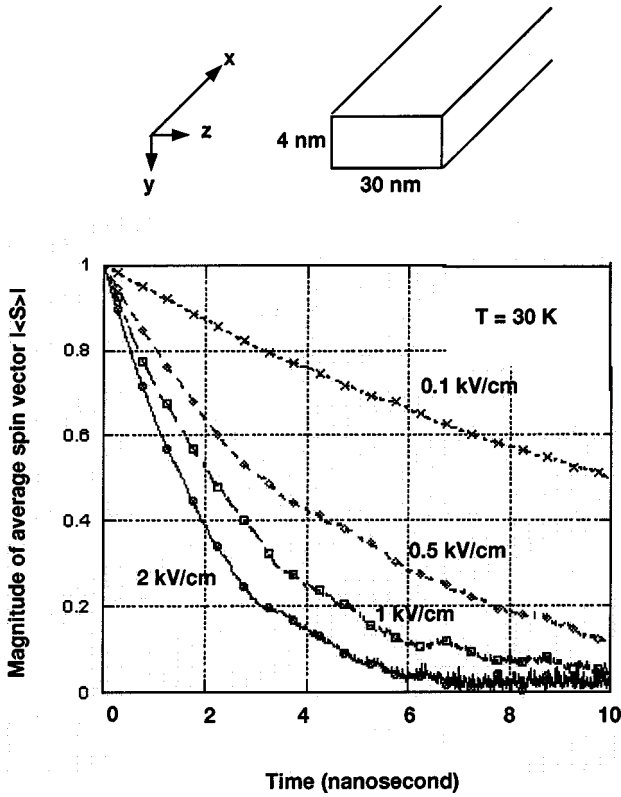
FIG. 1. Temporal dephasing of the ensemble average spin vector with time in a GaAs quantum wire of dimension 4 nm×30 nm at a lattice temperature of 30 K. The results are shown for various driving electric fields E. The spins are injected with their polarization initially aligned along the wire axis. The geometry of the wire and the axes designation are shown above.

axis of the quantum wire to induce charge flow. In addition, there is another transverse electric field E_y applied in the y direction that causes Rashba spin-orbit interaction. This configuration mimics the configuration of a spin interferometer proposed in Ref. 5.

Electrons are injected into this wire (from a half-metallic contact) with a specific spin polarization. We are interested in finding how the injected spin decays with time as the electron traverses the quantum wire under the action of the electric fields E_x and E_y while being subjected to elastic and inelastic scattering events.

Following Saikin *et al.*,[24] we treat the spin using the standard spin density matrix[32]

$$\rho_\sigma(t) = \begin{bmatrix} \rho \uparrow \uparrow (t) & \rho \uparrow \downarrow (t) \\ \rho \downarrow \uparrow (t) & \rho \downarrow \downarrow (t) \end{bmatrix}, \quad (1)$$

which is related to the spin polarization component as $S_n(t) = \mathrm{Tr}[\sigma_n \rho_\sigma(t)]$ $(n = x, y, z)$. Over a small time interval δt, we will assume that no scattering takes place and that the electron's momentum changes slowly enough due to the driving electric field (in other words $E_x \delta t$ is small enough) that transport can be described by a constant (time-independent) momentum or wave vector. We take this wave vector to be the average of the wave vector at the beginning and end of the time interval

$$k = (k_{\mathrm{initial}} + k_{\mathrm{final}})/2 = k_{\mathrm{initial}} + qE_x \delta t/2\hbar. \quad (2)$$

During this interval, the spin density matrix undergoes a unitary evolution according to

$$\rho_\sigma(t + \delta t) = e^{-iH_{\mathrm{SO}}(k)\delta t/\hbar} \rho_\sigma(t) e^{iH_{\mathrm{SO}}(k)\delta t/\hbar}, \quad (3)$$

where $H_{\mathrm{SO}}(k)$ is the momentum dependent spin-orbit interaction Hamiltonian that has two main contributions due to the bulk inversion asymmetry (Dresselhaus interaction)[33]

$$H_D(k) = -\beta \langle k_y^2 \rangle k \sigma_x \quad (k \equiv k_x) \quad (4)$$

and the structural inversion asymmetry (Rashba interaction)[34]

$$H_R(k) = -\eta k \sigma_z. \quad (5)$$

The Rashba term is present only if inversion symmetry in the structure is broken by some external agent such as the external electric field E_y. The constants β and η depend on the material and, in the case of η, also on the external electric field E_y breaking inversion symmetry.

Equation (3) describes a rotation of the spin vector about an effective magnetic field determined by the magnitude of the average wave vector during the time interval δt. Note that during this time interval, the spin dynamics is coherent and there is no "dephasing" since the evolution is unitary. However, there are two agents that ultimately cause dephasing. The first is the electric field E_x that changes the "average wave vector" from one time interval δt to the next. The second is the stochastic scattering that changes the "average wave vector" between two successive intervals (separated by a scattering event) randomly. These two causative agents produce a distribution of spin states that results in effective dephasing when one ensemble averages over the spins of many electrons. The evolution of the ensemble averaged spin polarization vector **S** ($= S_x \mathbf{u}_x + S_y \mathbf{u}_y + S_z \mathbf{u}_z$, where $\mathbf{u}_n$ is the unit vector along the n direction) can be viewed as coherent motion (rotation) and dephasing/depolarization (reduction in magnitude). This type of dephasing is the D'yakonov-Perel' relaxation[35] which is the dominant mechanism for dephasing in one-dimensional structures.

Generally, there are many causes of spin dephasing namely interactions with local magnetic fields caused by magnetic impurities, nuclei and spin orbit interaction. In our work, we have considered only the D'yakonov-Perel' dephasing due to spin-orbit interaction since it is, by far, the dominant mechanism in quantum wires of technologically important semiconductors such as GaAs (which is the material we consider in Sec. III). In addition to D'yakonov-Perel', another type of dephasing mechanism associated with spin-orbit coupling is the Elliott-Yafet relaxation[36] that causes a spin to flip randomly during a momentum relaxing collision. It comes about because in a compound semiconductor such as GaAs, which lacks inversion asymmetry, the Bloch states in the crystal are not eigenstates of the spin operator. Therefore, a "spin-up" state has some "spin-down" component and vice versa. Consequently, a momentum relaxing scattering event can flip spin. Fortunately, in a quantum wire structure, the momentum relaxing events are strongly suppressed

because of the one-dimensional constriction of the phase space for scattering.[37] Accordingly, the Elliott-Yafet mechanism is considerably weaker than the D'yakonov-Perel' mechanism in quasi-one-dimensional structures, and therefore can be ignored as a first approximation. Finally, there is one last important dephasing mechanism known as the Bir-Aronov-Pikus mechanism[38] accruing from exchange coupling between electrons and holes. This mechanism is absent in unipolar transport. In our simulations, we have considered only the D'yakonov-Perel' mechanism, but inclusion of the Elliott-Yafet mechanism is a relatively easy extension and is reserved for future work.

Returning to Eq. (3), the unitary evolution in time can be recast in the following equation for the temporal evolution of the spin vector:[3]

$$\frac{d\mathbf{S}}{dt} = \vec{\Omega} \times \mathbf{S}, \tag{6}$$

where the so-called "precession vector" $\vec{\Omega}$ has two contributions $\Omega_D(k)$ and $\Omega_R(k)$ due to the bulk inversion asymmetry (Dresselhaus interaction) and the structural inversion asymmetry (Rashba interaction), respectively:

$$\Omega_D(k) = \frac{2a_{42}}{\hbar} \left(\frac{\pi}{W_y} \right)^2 k,$$

$$\Omega_R(k) = \frac{2a_{46}}{\hbar} E_y k, \tag{7}$$

where a_{42} and a_{46} are material constants and W_y is the transverse dimension of the wire.

Christensen and Cardona[39] calculated a_{42} to be equal to 2.9×10^{-29} eV m^3 in GaAs, whereas Richards and Jusserand[40] deduced its value to be 1.6×10^{-29} eV m^3 from Raman experiments. In our simulations, we take the value to be 2×10^{-29} eV m^3. The value of a_{46} is taken to be 9×10^{-39} C m^2.[31] In our simulations, we assumed $E_y = 100$ kV/cm.

As stated before, we assume that over the short time interval δt, the electron's wave vector is time invariant and given by the average wave vector in Eq. (2). Consequently, the Ω's are constant and independent of time in the interval δt. Accordingly, the solution of Eq. (6) for the spin components yields

$$S_x(t+\delta t) = -\frac{\Omega_R}{\Omega_T} \left[S_y(t)\sin(\Omega_T \delta t) \right.$$

$$+ \left(\frac{\Omega_D}{\Omega_T} S_z(t) - \frac{\Omega_R}{\Omega_T} S_x(t) \right) \cos(\Omega_T \delta t) \right]$$

$$+ \left(\frac{\Omega_D}{\Omega_T} \right)^2 S_x(t) + \frac{\Omega_D \Omega_R}{\Omega_T^2} S_z(t),$$

$$S_y(t+\delta t) = S_y(t)\cos(\Omega_T \delta t)$$

$$+ \left(\frac{\Omega_R}{\Omega_T} S_x(t) - \frac{\Omega_D}{\Omega_T} S_z(t) \right) \sin(\Omega_T \delta t),$$

$$S_z(t+\delta t) = \frac{\Omega_D}{\Omega_T} \left[S_y(t)\sin(\Omega_T \delta t) \right.$$

$$+ \left(\frac{\Omega_D}{\Omega_T} S_z(t) - \frac{\Omega_R}{\Omega_T} S_x(t) \right) \cos(\Omega_T \delta t) \right]$$

$$+ \left(\frac{\Omega_R}{\Omega_T} \right)^2 S_z(t) + \frac{\Omega_D \Omega_R}{\Omega_T^2} S_x(t), \tag{8}$$

where $\Omega_T = \sqrt{\Omega_R^2 + \Omega_D^2}$. All Ω's are calculated at the average value of the wave vector in the interval δt given by Eq. (2). It is easy to verify from the above equations that spin is conserved for every individual electron, i.e.,

$$S_x^2(t+\delta t) + S_y^2(t+\delta t) + S_z^2(t+\delta t) = S_x^2(t) + S_y^2(t) + S_z^2(t)$$

$$= |\mathbf{S}|^2. \tag{9}$$

A. Monte Carlo simulation

From Eq. (8), we see that the temporal evolution of the spin in any time interval δt is governed by the spin precession vector. This vector changes from one time interval to the next because it depends on the electron wave vector [Eq. (7)] that dynamically evolves during transport. The time evolution of the wave vector is found from a Monte Carlo solution of the Boltzmann transport equation in a quantum wire.[41–43] Equation (8) is solved directly in the Monte Carlo simulator in each time interval δt. If a scattering event takes place in the middle of any such interval, the evolution of the spin according to Eq. (8) is immediately terminated, the wave vector state is updated depending on the type of scattering event that took place, the Ω's are recalculated based on the new wave vector, and the evolution of the spin is continued according to Eq. (8) for the remainder of the interval δt. At the end of every time interval δt, we collect statistics about the spin components.

The following scattering mechanisms are included in the Monte Carlo simulator: surface optical phonons, polar and nonpolar acoustic phonons, and confined polar optical phonons. A multi-subband simulation is employed; six subbands are considered in the z direction and only one in the y direction. This is justified since the width of the wire (z dimension) is assumed to be 30 mm and the thickness (y dimension) is only 4 nm. The energy separation between the closest two subbands is 6 meV (corresponding to a temperature of 52 K). At the highest lattice temperature (50 K) and electric field (4 kV/cm) considered in our simulations, we find that the lowest four subbands are occupied while the highest two subbands do not contain any electron. No intervalley transfer (from the Γ valley to the L valley takes place). The details of the simulator can be found in Refs. 42, 43.

Equations (8) are solved directly in the Monte Carlo simulator. We use a time step δt of 10 fs and a 1000–10 000 electron ensemble to collect spin statistics. We find the magnitude of the spin vector $\mathbf{S}$ as a function of time, as well as the components S_x, S_y, and S_z as functions of time. At the end of the simulation, we find the distribution of S_x, S_y, and S_z calculated over the electron ensemble.

TABLE I. Spin dephasing times as a function of driving electric field in a GaAs quantum wire of dimensions $30 \text{ nm} \times 4 \text{ nm}$ at a temperature of 30 K. The spins are initially polarized *along* the wire axis.

Electric field (kV/cm)	Spin dephasing time (sec)
0.1	1.7×10^{-8}
0.5	5.0×10^{-9}
1.0	3.5×10^{-9}
2.0	2.5×10^{-9}

III. RESULTS AND DISCUSSION

We consider two cases: electrons are injected with their spins initially (i) polarized along the axis of the quantum wire and (ii) polarized transverse to the axis of the quantum wire. We call these two cases x-polarized injection and y- (or z-) polarized injection, respectively. In the results to follow, we show that the spin dynamics is drastically different for the two cases. In other words, there is significant anisotropy.

A. *x*-polarized injection

We first consider the case of x-polarized injection. All electrons are injected with their spins completely polarized along the axis of the wire.

1. Effect of driving electric field

In Fig. 1, we show how the magnitude of the average (ensemble averaged over all electrons) spin vector **S** decays with time for four different values of the longitudinal electric field E_x applied along the axis of the wire. This field drives transport. The lattice temperature is 30 K.

From Fig. 1, we see that the decay is nearly exponential. Therefore, we will define the spin dephasing time as the time it takes for $|\langle \mathbf{S} \rangle|$ to decay to $1/e$ times its initial value of 1. Table I shows the spin dephasing time as a function of electric field.

As expected, the dephasing time decreases with increasing electric field. There are two contributing factors for this trend. First, the average wave vector k given by Eq. (2) changes more rapidly from one time interval to another with increasing electric field E_x. Hence the precession vector Ω_T which depends on k changes more rapidly from one time interval to another at a higher electric field. Now consider the random effect of scattering which results in different initial wave vector k_{initial} for different electrons in a given time interval. This results in different k (and hence different Ω's, or different precession rates) for different electrons in the same time interval. Ensemble averaging over the electrons therefore causes the magnitude of the spin vector **S** to decay, resulting in effective spin dephasing (or depolarization). Since the difference between the precession rates for different electrons will be larger at a stronger electric field E_x, the dephasing rate increases with increasing electric field. The second factor that contributes to this trend is that the frequency of scattering itself increases with increasing electric field. Scattering randomizes the Ω's since it randomizes k.
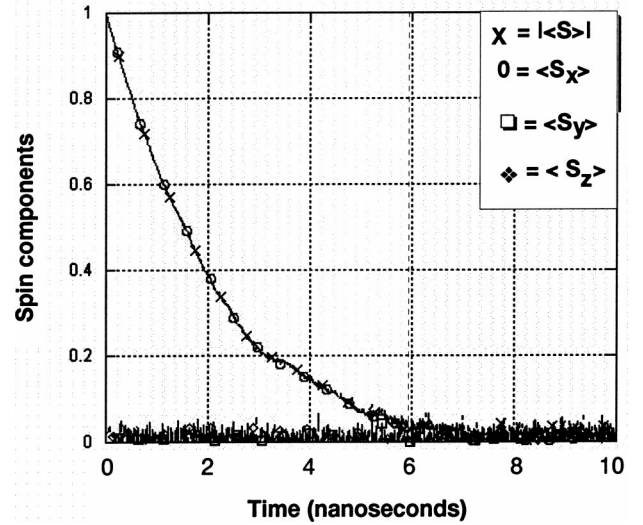
FIG. 2. Temporal dephasing of the x, y, and z components of ensemble average spin in the same GaAs wire at 30 K. The driving electric field is 2 kV/cm and the spins are injected with their polarization initially aligned along the wire axis.

This also results in faster dephasing at stronger electric fields.

At first glance, it may be troubling to assimilate the fact that the magnitude of the ensemble averaged $\mathbf{S}(=|\langle \mathbf{S} \rangle|)$ can decay with time. One should remember that the magnitude of $\mathbf{S}(=|\mathbf{S}|)$ is conserved only for an *individual* electron as shown by Eq. (9), but the magnitude is not invariant when we ensemble average over *many* electrons. It is this ensemble averaging that results in effective spin dephasing, as mentioned before.

2. Temporal decay of spin components

In Fig. 2 we show how the average (ensemble averaged over all electrons) x, y, and z, components of the spin decay with time. The driving electric field $E_x = 2$ kV/cm and the lattice temperature is 30 K. Since, initially the spin was polarized along the x direction, the ensemble averaged y and z components remain near zero and the ensemble averaged x component decays with time. The decay of the ensemble averaged x-component is indistinguishable from the decay of $|\langle \mathbf{S} \rangle|$ shown in Fig. 1, as expected.

3. Spin distribution

In Figs. 3(a)–3(c), we show the distribution of the x, y, and z components of the spins in the electron ensemble once steady state is reached. Again, the driving electric field is 2 kV/cm and the lattice temperature is 30 K. There is a slight depletion at the extremities of the distribution function $(S_x, S_y, S_z = \pm 1)$, but otherwise, these are uniform flat-topped distributions showing that all values of spin components are equally likely. Of course, the nonsteady-state (transient) distribution does not behave this way. To illustrate this point, we show in Fig. 3(d), the distribution of the x component 10 ns after injection. The electric field in this case is 0.1 kV/cm and obviously (as can be seen from Fig. 1) steady
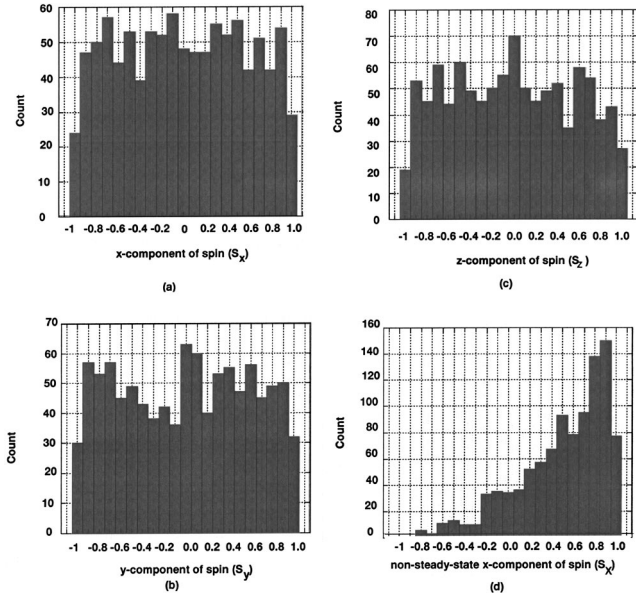
FIG. 3. Distribution of the spin components in the GaAs wire. The driving electric field is 2 kV/cm and the lattice temperature is 30 K. Spins are injected with their polarization initially aligned along the wire axis. (a) Steady state distribution of the x component, (b) steady state distribution of the y component, (c) steady state distribution of the z component, and (d) transient distribution (after a time of 10 ns) of the x component when the driving electric field is 0.1 kV/cm.

FIG. 4. Temperature dependence of the spin dephasing in the GaAs wire when the driving electric field is 2 kV/cm. Spins are injected with their polarization initially aligned along the wire axis.

state has not been reached. In this case, the distribution is still skewed heavily towards the initial distribution at time $t=0$ when all electrons had an x component equal to $+1$. When steady state is reached, $|\langle\mathbf{S}\rangle|$ will decay nearly to zero and the distribution will become more or less uniform and flat topped.

4. Effect of temperature

In Fig. 4, we show how the dephasing rate and the decay characteristic of $|\langle\mathbf{S}\rangle|$ depends on the lattice temperature. Increasing lattice temperature results in increasing phonon scattering that randomizes k and Ω's more rapidly. This results in faster dephasing. In the temperature range considered here (4.2–30 K), most of the scattering is due to spontaneous emission of phonons (which is temperature independent), as opposed to stimulated emission or absorption (which are temperature dependent). Therefore, it is no surprise that the decay rate and characteristics are weakly sensitive to temperature in this range.

In Figs. 5(a)–5(c), we show the steady state distributions of the spin components at a lattice temperature of 4.2 K. The driving electric field is 2 kV/cm. Comparing with Fig. 3, we see that the steady state distributions look very similar so that the temperature does not significantly affect them. Additionally, although not shown, we have found that the shape of the steady state distribution is independent of the driving electric field.

B. Y- or z-polarized injection

We now consider injection with the initial spins polarized transverse to the wire axis. There is a slight difference be-

tween injecting spins polarized along the y direction versus the z direction since the structure is both geometrically asymmetric (z dimension is larger than the y dimension) and also electrically asymmetric (there is an electric field E_y along the y direction to induce Rashba spin orbit coupling). Indeed these differences result in slight differences between y- and z-polarized injections, but they are small.
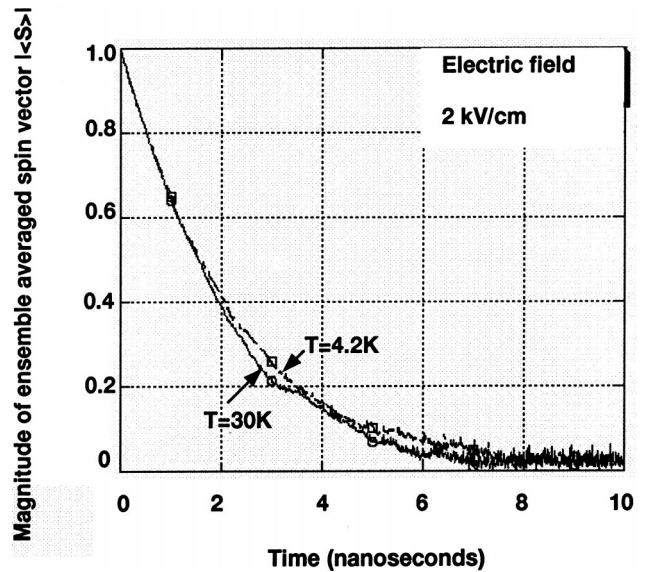
1. Effect of driving electric field

In Fig. 6(a), we show the temporal dephasing characteristics of $|\langle\mathbf{S}\rangle|$ for six different electric fields when electrons are initially polarized along the z direction. The lattice temperature is 30 K as before. Again, the spin dephases faster at higher electric fields as expected. But now, comparison of Figs. 1 and 6 reveal that the dephasing rates are very "anisotropic" in the sense that the dephasing rates are different by more than an order of magnitude depending on whether the spins are initially polarized along the wire or transverse to the wire. The dephasing rate is faster when the initial spins are polarized transverse to the wire axis. One obvious reason for this is that in a quasi-one-dimensional structure, the Dresselhaus spin orbit interaction is inoperative on spin polarized along the axis of the wire. Therefore, x-polarized spin dephases only due to the Rashba interaction in the quantum wire, while the y- and z-polarized spins dephase due to both the Rashba and the Dresselhaus interactions. Consequently, y- and z-polarized spins dephase faster. The spin dephasing times for various electric fields are shown in Table II.

In Fig. 6(b), we show the spin dephasing characteristics when the spins are initially polarized along the y direction. The dephasing time at an electric field of 2 kV/cm is now 0.25 ns compared to 0.1 ns when the initial polarization is along the z direction. This difference (a factor of 2.5) is expected since the structure is both geometrically and electrically asymmetric with respect to y and z, as stated before.

(a)

(b)

(c)
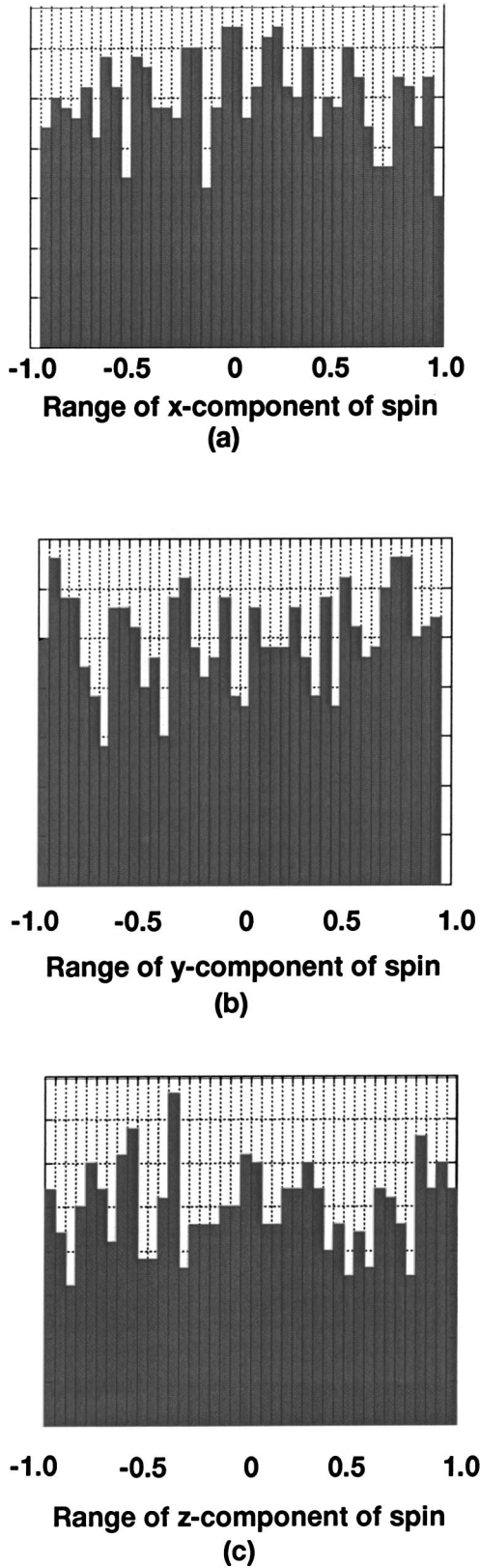
FIG. 5. Steady state distribution of the spin components in the GaAs wire. The driving electric field is 2 kV/cm and the lattice temperature is 4.2 K. Spins are injected with their polarization initially aligned along the wire axis. (a) Distribution of the x component, (b) distribution of the y component, and (c) distribution of the z component.

(a)
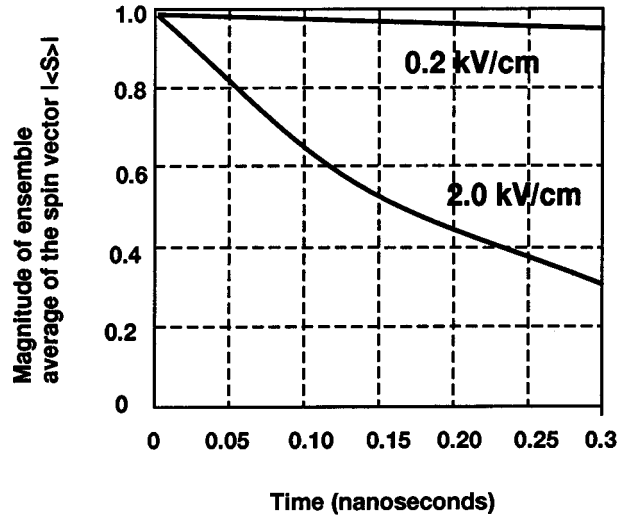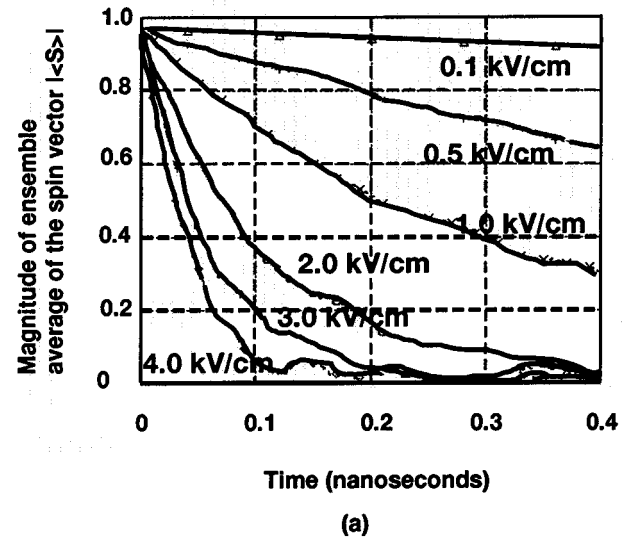
FIG. 6. Temporal dephasing of the ensemble average spin vector with time in a GaAs quantum wire of dimension 4 nm×30 nm at a lattice temperature of 30 K. The results are shown for various driving electric fields E. (a) The spins are injected with their polarization initially aligned along the z axis which is mutually perpendicular to the wire axis and the direction of the electric field E_y used to induce the Rashba spin orbit coupling; (b) spins are injected with their polarization initially aligned along the y axis which is the direction of the electric field E_y used to induce the Rashba spin orbit coupling.

From Figs. 1 and 6, we find that the electric field dependence of the spin dephasing rate is stronger when the spins are initially injected with polarization transverse to the wire axis. Comparing Tables I and II, the difference between the dephasing rates at fields of 0.1 kV/cm and 2 kV/cm is a factor of ~7 when spins are initially polarized along the wire axis, while it is a factor of 50 when the initial polarization is transverse to the wire axis. This difference too can be attributed to the fact that both Rashba and Dresselhaus interactions are operative on the initial spin for transverse injection (while only the former is operative for longitudinal injection)

TABLE II. Spin dephasing times as a function of driving electric field in a GaAs quantum wire of dimensions $30 \, \text{nm} \times 4 \, \text{nm}$ at a temperature of 30 K. The spins are initially polarized *transverse to the wire axis.*

Electric field (kV/cm)	Spin dephasing time (sec)
0.1	5.0×10^{-9}
0.5	9.0×10^{-10}
1.0	3.0×10^{-10}
2.0	1.0×10^{-10}
3.0	6.0×10^{-11}
4.0	4.0×10^{-11}

so that the electric field is more effective for the transverse case.

In Fig. 6, there is a nearly discrete change in the value of $|\langle \mathbf{S} \rangle|$ at $t = 0$ (it is even more pronounced in Fig. 10; see later). This is a numerical artifact. Our model is based on the assumption that the Ω's are constant in the time interval δt and correspond to the average k within that time interval [as given by Eq. (2)]. This is a good assumption when δt is small enough. If δt is too large, the assumption is no longer reasonable and artificial features can be manifested in the simulation results such as the discrete jump at $t = 0$. We have verified that this artifact diminishes when we make δt smaller. We have used $\delta t = 10$ fs in our simulations. Using a smaller value of δt reduces the artifact, but increases the computational time. Therefore, we have chosen a value of δt that is a compromise between accuracy and computational resources. Similar numerical artifacts were present in the simulations of Ref. 24.

2. Decay of spin components

In Fig. 7(a) we show how the average (ensemble averaged over all electrons) x, y, and z components of the spin decay with time for z-polarized injection. The driving electric field $E_x = 2$ kV/cm and the lattice temperature is 30 K. Since, initially the spin was polarized along the z direction, the ensemble averaged x component remains near zero since the Dresselhaus interaction does not couple [see Eq. (8)] y- or z-polarized spins to the x-polarized spins. Only the Rashba interaction couples to the x-polarized spins (if the Rashba interaction were absent, the x component of the spin will remain identically zero for every electron). Any nonzero value of the x component at any time is only because of the Rashba interaction. Since this interaction is weak in our case, the x component remains near zero. The y and z components of the spin oscillate with time [in accordance with Eq. (8)] with a slowly decaying envelope. They start out with a $\pi/2$ phase shift between them initially which quickly changes owing to dephasing (or ensemble averaging over electrons).

In Fig. 7(b), we show the same characteristics for y-polarized injection. There are slight differences between Figs. 7(a) and 7(b), again owing to the fact that the structure is geometrically and electrically asymmetric with respect to y and z.
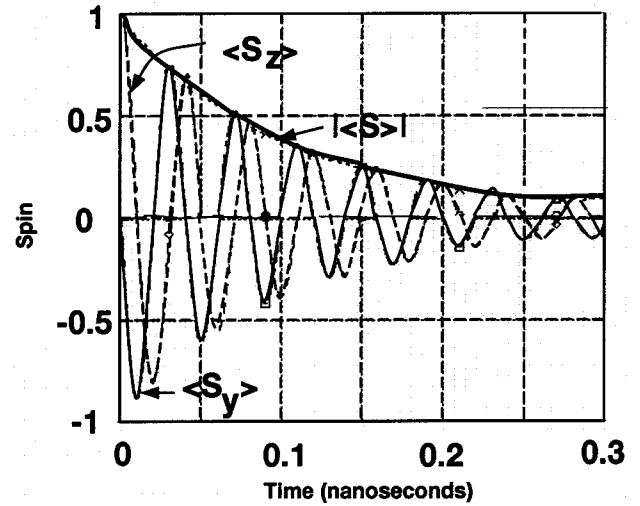
(a)
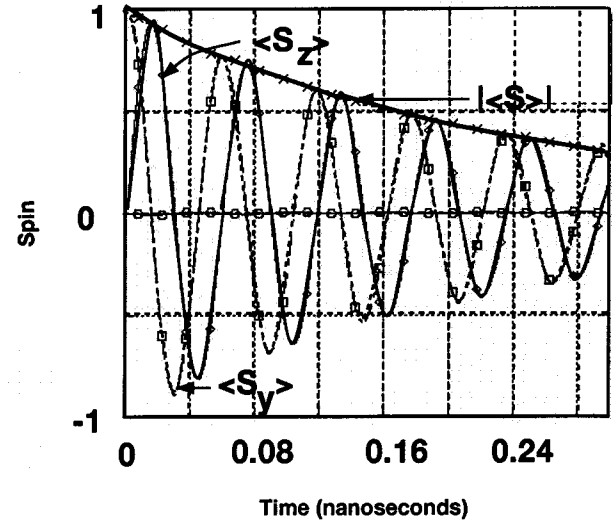
FIG. 7. Temporal dephasing of the x, y, and z components of ensemble average spin in the GaAs wire at 30 K. The driving electric field is 2 kV/cm and the spins are injected with their polarization initially aligned along the (a) z direction and (b) y direction. The x component remains zero throughout, while the y and z components oscillate, starting with a $\pi/2$ phase shift between themselves.

It is interesting to note that the temporal decay of the x component in Figs. 1 and 2 is monotonic (with no hint of any oscillatory component), while the temporal decay of the y and z components in Fig. 7 is clearly oscillatory. The oscillatory component is a manifestation of the coherent dynamics (spin rotation) while the monotonic decay is a result of the incoherent dynamics (spin dephasing or depolarization). There is a competition between these two dynamics determined by the relative magnitudes of the spin precession vector and the dephasing rate. For the x component, the spin precession vector is small because it is solely due to the Rashba interaction which is weak. Hence the dephasing dynamics wins handsomely resulting in no oscillatory component. In contrast, the spin precession vector for the y and z components is much larger since it is the result of both
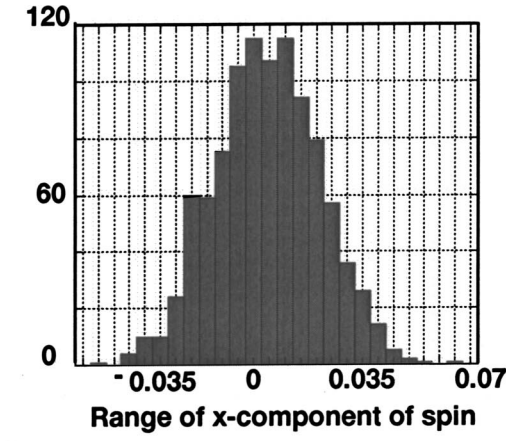
(a)
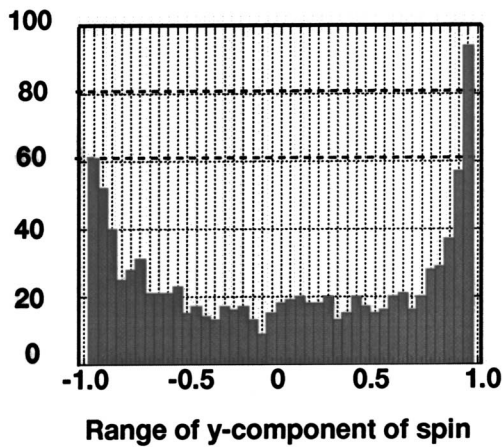
(b)
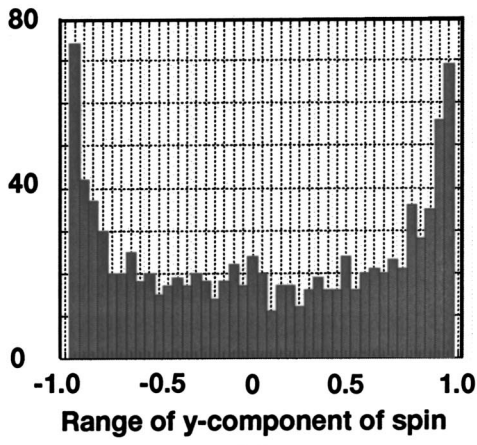
(c)

FIG. 8. Steady state distribution of the spin components in the GaAs wire. The driving electric field is 2 kV/cm and the lattice temperature is 30 K. Spins are injected with their polarization initially aligned along the z axis. (a) Distribution of the x component, (b) distribution of the y component, and (c) distribution of the z component.
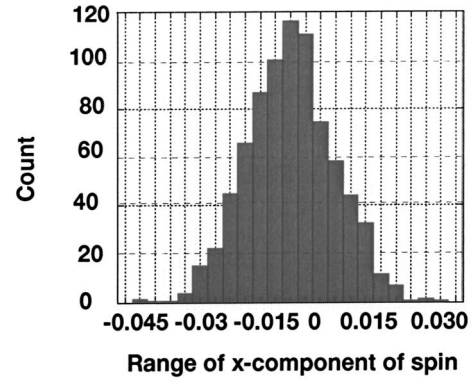
(a)
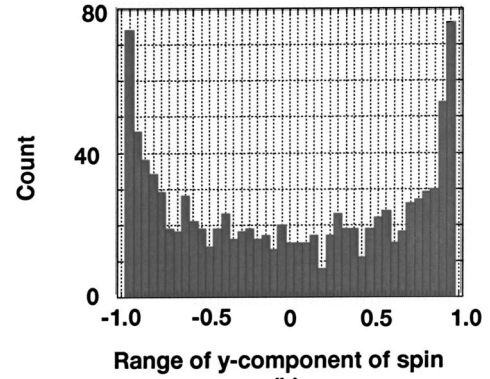
(b)
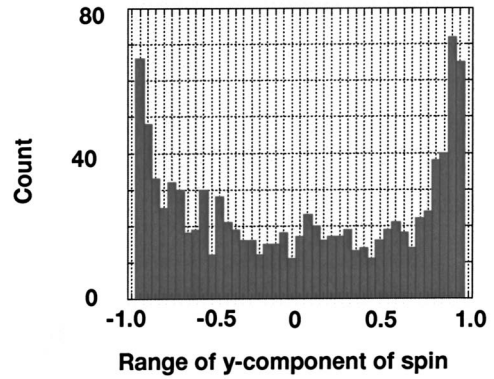
(c)

FIG. 9. Steady state distribution of the spin components in the GaAs wire. The driving electric field is 2 kV/cm and the lattice temperature is 30 K. Spins are injected with their polarization initially aligned along the y axis. (a) Distribution of the x component, (b) distribution of the y component, and (c) distribution of the z component.

Dresselhaus (bulk inversion asymmetry) and Rashba (structural inversion asymmetry) interactions. Consequently, the oscillatory component is visible in the decays characteristics of the y and z components, but not in the case of the x component.

3. Spin distributions

In Figs. 8(a)–8(c), we show the distribution of the x, y, and z components of the spins in the electron ensemble
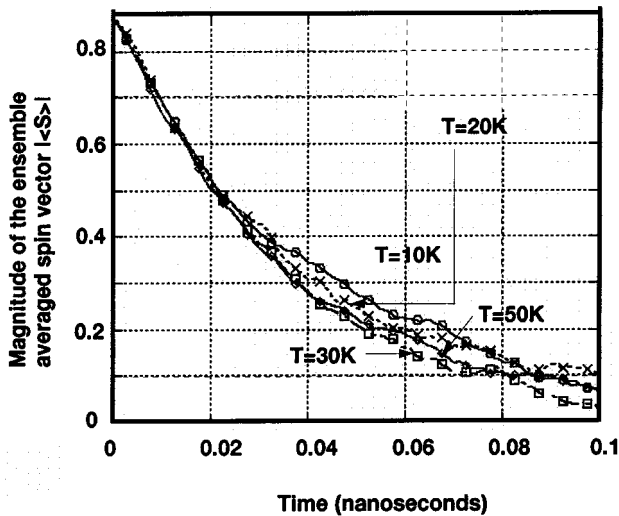
FIG. 10. Temperature dependence of the spin dephasing in the GaAs wire when the driving electric field is 2 kV/cm. Spins are injected with their polarization initially aligned along the z axis. There is no clearly discernible temperature dependence in the range of 10–50 K within the stochastic fluctuations of Monte Carlo simulation.

once steady state is reached. We define steady state as the condition when $|\langle\mathbf{S}\rangle|$ approaches zero in Fig. 7. Again, the driving electric field is 2 kV/cm and the lattice temperature is 30 K. Comparing these figures to Figs. 3(a)–3(c), we find that the steady state distributions are vastly and qualitatively different for injection with transverse polarization compared to injection with longitudinal polarization. The distributions in Fig. 8 are not uniform flat topped distributions at all.

The x component shows a very narrow Gaussian-type distribution with zero mean and a standard deviation less than 0.03. This is expected since the x component should be ideally zero (the distribution would be a delta function at zero) in the absence of the Rashba interaction. The Rashba interaction causes some spread about the zero value, but the Rashba interaction is weak and therefore the spread is small.

The y and z components show a U-shaped distribution weighted towards the extreme values of −1 and +1. This U shape is a consequence of the oscillatory nature of the decay characteristics for y and z components seen in Fig. 7. Note that the slopes of the decay characteristics are zero at the peaks and valleys when the spins have close to their extremal

values. Hence the spins spend more time near their extremal values. Consequently, more spins in the ensemble will have values close to −1 and +1 than any other intermediate value.

In Figs. 9(a)–9(c), we show the steady state spin distributions when spins are initially polarized along the y direction. There is a slight difference between the distributions in Figs. 8 and 9 because of the geometric and electrical asymmetry between y and z. Otherwise, the qualitative features are the same.

For both y- and z-polarized injections, we have found that the shapes of the steady state distributions are fairly independent of temperature and driving electric field.

4. Effect of temperature

Finally, in Fig. 10, we show the effect of temperature on the dephasing (or depolarization) characteristics of $|\langle\mathbf{S}\rangle|$ when spins are initially polarized along the z direction. Once again, the driving electric field is 2 kV/cm. There is a very weak temperature dependence in the range 10–50 K for essentially the same reason as alluded to in Sec. III A 4.

IV. CONCLUSION

In this paper, we have studied spin dephasing in a quasi-one-dimensional structure. The dephasing rate was found to be strongly anisotropic in the sense that it depends sensitively on whether the spins are initially polarized along the wire axis or perpendicular to the wire axis. Anisotropic effects were also observed in Ref. 24. A somewhat different type of anisotropy in the spin relaxation rates was discussed in Ref. 44 and was attributed to interference between various types of spin-orbit interactions. In our case, the anisotropy is primarily due to the fact that the Dresselhaus interaction operates only on spins polarized transverse to the wire axis and not on spins polarized along the wire axis. This anisotropy can be exploited in the design of spintronic devices such as the gate controlled spin interferometer where the suppression of spin dephasing is a critical issue. We have also shown that the steady state spin distributions are strongly a function of the initial polarization. The dephasing rate has a very weak dependence on temperature and a moderately strong dependence on the driving electric field.

*E-mail address: sbandy@vcu.edu

[1] G. Prinz and K. Hathaway, Phys. Today **48**, 24 (1995); G. Prinz, Science **270**, 1660 (1998).

[2] S. A. Wolf, D. D. Awschalom, R. A. Buhrman, J. M. Daughton, S. von Molnar, M. L. Roukes, A. Y. ChtChelkanova, and D. M. Treger, Science **294**, 1488 (2001).

[3] D. D. Awschalom, M. E. Flatte, and N. Samarth, Sci. Am. **286**, 66 (2002).

[4] S. Das Sarma, Am. Sci. **89**, 516 (2001).

[5] S. Datta and B. Das, Appl. Phys. Lett. **56**, 665 (1990).

[6] M. E. Flatte and G. Vignale, Appl. Phys. Lett. **78**, 1273 (2001).

[7] I. Zutic, J. Fabian, and S. Das Sarma, Appl. Phys. Lett. **79**, 1558 (2001).

[8] T. Koga, J. Nitta, H. Takayanagi, and S. Datta, Phys. Rev. Lett. **88**, 126601 (2002).

[9] X. F. Wang, P. Vasilopoulos, and F. M. Peeters, Phys. Rev. B **65**, 165217 (2002).

[10] S. Bandyopadhyay and V. P. Roychowdhury, Superlattices Microstruct. **22**, 411 (1997).

[11] V. Privman, I. D. Vagner, and G. Kventsel, Phys. Lett. A **239**, 141 (1998).

[12] B. E. Kane, Nature (London) **393**, 133 (1998).

[13] S. Bandyopadhyay, Phys. Rev. B **61**, 13813 (2000).

[14] G. Feher, Phys. Rev. **114**, 1219 (1954).

[15] J. M. Kikkawa and D. D. Awschalom, Phys. Rev. Lett. **80**, 4313 (1998).

[16] P. Mohanty, J. M. Q. Jariwalla, and R. A. Webb, Phys. Rev. Lett. **78**, 3366 (1997).

[17] F. Mireles and G. Kirczenow, Phys. Rev. B **64**, 024426 (2001).

[18] Th. Schapers, J. Nitta, H. B. Heersche, and H. Takayanagi, Physica E **13**, 564 (2002).

[19] T. Matsuyama, C.-M. Hu, D. Grundler, G. Meier, and U. Merkt, Phys. Rev. B **65**, 155322 (2002).

[20] M. Cahay and S. Bandyopadhyay, cond-mat/0305622 (unpublished).

[21] J. Fabian, I. Zutic, and S. Das Sarma, Phys. Rev. B **66**, 165301 (2002).

[22] G. Schmidt and L. W. Molenkamp, Semicond. Sci. Technol. **17**, 310 (2002).

[23] Z. G. Yu and M. E. Flatté, Phys. Rev. B **66**, 235302 (2002).

[24] S. Saikin, M. Shen, M. C. Cheng, and V. Privman, cond-mat/0212610 (unpublished); M. Shen, S. Saikin, M. C. Cheng, and V. Privman, cond-mat/0302395 (unpublished).

[25] W. H. Lau, J. T. Olesberg, and M. E. Flatté, Phys. Rev. B **64**, 161301 (2001).

[26] M. S. Lundstrom, *Fundamentals of Carrier Transport*, Vol. x of *Modular Series on Solid State Devices* (Addison-Wesley, Reading, MA, 1990).

[27] G. Schmidt, C. Gould, P. Grabs, A. M. Lunde, G. Richter, A. Slobodsky, and L. W. Molenkamp, cond-mat/0206347 (unpublished).

[28] H. Sanada, Y. Arata, Y. Ohno, Z. Chen, K. Kayanuma, Y. Oka, F. Matsukura, and H. Ohno, Appl. Phys. Lett. **81**, 2788 (2002).

[29] M. Q. Weng and M. W. Wu, J. Appl. Phys. **93**, 410 (2003).

[30] Y. Qi and S. Zhang, Phys. Rev. B **67**, 052407 (2003).

[31] A. Bournel, P. Dollfus, S. Galdin, F-X. Musalem, and P. Hesto, Solid State Commun. **104**, 85 (1997); A. Bournel, P. Dollfus, P. Bruno, and P. Hesto, Mater. Sci. Forum **297−298**, 205 (1999); A. Bournel, V. Delmouly, P. Dollfus, G. Tremblay, and P. Hesto, Physica E (Amsterdam) **10**, 86 (2001).

[32] K. Blum, *Density Matrix Theory and Applications* (Plenum, New York, 1996).

[33] G. Dresselhaus, Phys. Rev. **100**, 580 (1955).

[34] E. I. Rashba, Sov. Phys. Semicond. **2**, 1109 (1960); Y. A. Bychkov and E. I. Rashba, J. Phys. C **17**, 6039 (1984).

[35] M. I. D'yakonov and V. I. Perel', Sov. Phys. Solid State **13**, 3023 (1972).

[36] R. J. Elliott, Phys. Rev. **96**, 266 (1954).

[37] H. Sakaki, Jpn. J. Appl. Phys. **19**, L735 (1980).

[38] G. L. Bir, A. G. Aronov, and G. E. Pikus, Sov. Phys. JETP **42**, 705 (1976).

[39] N. E. Christensen and M. Cardona, Solid State Commun. **51**, 491 (1984).

[40] D. Richards and B. Jusserand, Phys. Rev. B **59**, R2506 (1999).

[41] D. Jovanovich and J-P. Leburton, in *Monte Carlo Device Simulation: Full Band and Beyond*, edited by K. Hess (Kluwer Academic, Boston, 1991), pp. 191−218.

[42] N. Telang and S. Bandyopadhyay, Appl. Phys. Lett. **66**, 1623 (1995).

[43] N. Telang and S. Bandyopadhyay, Phys. Rev. B **51**, 9728 (1995).

[44] N. S. Averkiev, L. E. Golub, and M. Willander, Fiz. Tekh. Poluprovodn. (S.-Peterburg) **36**, 97 (2002) [Semiconductors **36**, 91 (2002)].